Real-time extraction of the respiratory rate from photoplethysmographic signals using wearable devices

Roxana Alexandra Cernat[1,2], Constantin Ungureanu[2,3], Georgeta Mihaela Ungureanu[1], Ronald Aarts[2,4], Johan Arends[2,3]

1. Faculty of Medical Engineering, University Politehnica of Bucharest, Romania;
2. Dept. of Electrical Engineering , Eindhoven University of Technology, The Netherlands;
3. Academic Center of Epileptology, Kempenhaeghe, Heeze, The Netherlands;
4. Philips Research Eindhoven, The Netherlands

Abstract

The respiratory rate is considered one of the vital signs. Its real-time assessment in real-time is valuable information for clinicians, especially in conditions like epilepsy, sleep apnea or pulmonary disease. Current monitoring devices require a nasal cannula, a mask, or a chest band to determine the respiratory rate, which can cause discomfort to the patient, and can be difficult to handle in emergency cases of emergency. We investigated the potential of photoplethysmography (PPG) to determine the respiratory rate, which is an easy-to-use and comfortable method. We investigated the potential of 12 features, derived from infrared and green PPG signals, to determine the respiratory rate. The features include the commonly used pulse width variability (PWV) or pulse amplitude variability (PAV). We showed that a new feature introduced by us provides similar results as PWV and PAV on the Capnobase database. Furthermore, we developed a data fusion model that uses five different PPG features to obtain the respiratory rate in real-time. We evaluated this real-time system against a thermistor respiratory circuit. The error was less than 2 breaths per minute in the 6-30 breaths/minute range. Our system successfully computed the respiratory rate when the sensor was placed on different body locations such as the upper arm, the wrist and the ankles.

1 Introduction

The respiratory rate is defined as the number of breaths a person takes during a one-minute period of time and is measured while the subject is at rest. As one of the main vital signs, an accurate recording of the respiratory rate is important in predicting some serious medical events such as cardiac arrest, admission to the intensive care unit [1] or pneumonia [2].

In general, children have faster respiratory rates than adults [3]. The normal respiratory range for an adult is between 12-20 breaths per minute [3]. Both, an increased and decreased respiratory rate could be signs that something is wrong in our body. An

increased respiratory rate (tachypnea) could be caused by fever, dehydration, an asthma attack, infections or lung conditions, while the possible causes of a decreased respiratory rate (bradypnea) could be use of narcotics, alcohol, sleep apnea and brain conditions [4].

Monitoring the respiratory rate is also important in people suffering from epilepsy. The respiratory rate could reach abnormal values during an epileptic seizure but also before and after the seizure [5]. For example, during a tonic seizure respiration can stop (apnea) because of contraction of the respiratory muscles.

More recent studies have suggested that Sudden Unexplained Death in Epilepsy (SUDEP) could be caused by a combination of severe alteration of respiratory and cardiac functions, increased fluid in the lungs, and prone position [6, 7].

There are different methods for monitoring the respiratory rate of a subject. These methods are divided into contact and non-contact methods, indicating whether the device has to be in contact with the body of the subject or not [1]. Most common contact methods are based on detecting the chest and abdominal movement or measuring direct airflow through the mouth or nose. The main disadvantage of contact methods is that some patients may not feel comfortable with a device like a nasal cannula, mouth mask, ECG electrodes [8] or a strap around the chest.

There is a need to develop more unobtrusive yet accurate devices to monitor the respiratory rate in ambulatory settings. One of the possible modalities is photoplethysmography (PPG). In literature it is shown that respiration can induce changes in the pulse wave morphology recorded with a pulse oximeter [2, 9].

The extraction of the respiratory rate from the PPG signal has been achieved by several methods. Most studies use the Fast Fourier Transform (FFT) [10-12], but this requires a long time period to process the data. Digital filtering methods described by Nilsson et al. [13, 14] and Nakajima et al. [15], as well as the wavelet decomposition described by Addison et al. [16, 17], are other methods that have been used. Nilsson et al. proposed the use of a 3rd order Butterworth band-pass filter in their study, with a pass-band 0.1-0.3Hz, corresponding to 6-18 breaths per minute. They reported an average error of less than 0.5 breaths per minute. Addison et al. [16] developed a complex Matlab algorithm, using the wavelet transform to extract a breathing waveform from the PPG signal with an average error about 1 breath per minute. Better results have been obtained using an autoregressive (AR) modeling method [18], for which the mean error is 0.04.

Another approach presents the possibility of extracting respiratory information from derived PPG features, such as pulse width variability (PWV), pulse amplitude variability (PAV), pulse rate variability (PRV) and the PPG pulse envelope [2, 11, 19]. Lazaro et al. [19] presented in their paper a method to estimate the respiratory rate from PAV, PWV, and PRV using a spectrum-based algorithm [20]. The respiratory rate was extracted from the presented features independently, and also after a data fusion of these features [2, 19].

The respiratory rate modulates the PPG signal in three ways. For example, the pulse wave amplitude is affected by blood vessels flexibility. During expiration our blood vessels are more flexible than during inspiration [19]. Also, the intrathoracic pressure causes variation of pulse envelope and a decrease in cardiac output influ-

ences the pulse amplitude of PPG signal [2]. Changes in intrathoracic pressure during inspiration lead to decreased pulse amplitude during this phase of respiration [9]. Decreases in intrathoracic pressure lead to increasing venous return during inspiration. The baseline is modulated according to these changes [9].

The majority of the studies related to the extraction of the respiratory rate from PPG signals use measurements obtained from the finger, forehead, earlobe or forearm [10-13, 19, 21].

One aim of our research is to identify if other respiratory features can be derived from the PPG signal. The second one is to develop a system which enables us to estimate the respiratory rate in real-time from the PPG signal obtained from a reflection pulse oximeter device. The following sections describe the features, circuits, and methodology used to address the points presented above.

2 Materials and methods

2.1 Photoplethysmography theory

Pulse oximetry is a non-invasive method for measuring the heart rate (HR) and the arterial hemoglobin oxygen saturation (SpO_2). This device is an optical sensor made of two elements: a light source, typically a light-emitting diode (LED), to illuminate a region of tissue, and a photodetector (PD) to measure the amount of light exiting the tissue. A pulse oximeter is based on spectral analysis and combines two technologies: spectrophotometry (measurement of light intensity depending on color, or more specifically, depending on the wavelength of light) and photoplethysmography (PPG) (changes in blood volume in a given region of tissue) [22, 23].

Oxyhaemoglobin (HbO_2) and reduced haemoglobin (RHb) have different absorption characteristics for red and infrared light [24]. RHb has a higher optical extinction in the red region of the light spectrum, around 660 nm, compared to HbO_2. In the near-infrared region, around 940 nm, the opposite happens, where HbO_2 absorbs light stronger than RHb [25, 26].

The PPG waveform consists of two components: the AC component, also called the pulsatile component, of which the fundamental frequency is the heart rate [27], and the DC component or non-pulsatile component. The DC component is a result of the light absorption by skin, tissue, bone, venous blood and nonpulsatile arterial blood and varies slowly with the respiration, vasomotor activity, thermoregulation and Mayer waves [26, 28].

Most commercial pulse oximeters work in transmission mode, but the disadvantage of these is the fact that they are limited to several specific locations on the body, such as the fingertips, ear lobes and toes. For this reason, the interest has increased in developing a reflective pulse oximeter that can be used to obtain an accurate PPG measurement from more locations on the body [29, 30].

2.2 Pulse oximeter device

For our application we used the reflection mode pulse oximeter developed by Silvia et al [31]. This system comprises two red and two infrared (IR) LEDs, and two photodiodes, one for each wavelength. In this setup the light is sent at an incidence angle of 25^{o} (Fig. 1).

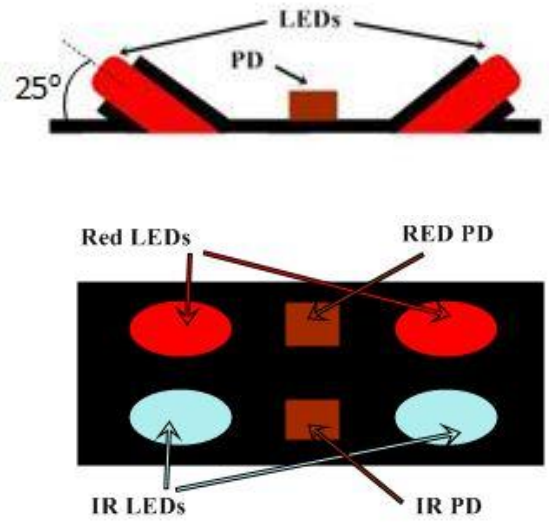

Fig. 1. Pulse oximeter setup

Silvia et. al [31] have shown that PPG signals could be recorded from different locations of the body like upper arm, forearm, wrist and ankle.

The optical setup is connected to the Easy Pulse boards (*http://embedded-lab.com/blog/?p=5508)*. The standard board presents a High Pass Filter (HPF) and a Low Pass Filter (LPF) with a cut-off frequency of 0.5 Hz and 3.4 Hz. We modified the cut-off frequency of the HPF from 0.5 Hz to 0.1 Hz in order to enable capturing respiratory rates as of 6 breaths per minute. The analog output from the Easy Pulse board was connected to an analog input from the expansion board, which is further connected to a Shimmer sensor node. The Shimmer unit can transmit data in real-time to a PC via Bluetooth. Further, we can process the data in real-time.

In order to determine the respiratory rate we used the PPG signal from the IR channel, whose amplitude is higher, when compared to the amplitude of the red PPG.

As a comparison, the respiratory rate was also determined from a green PPG signal, obtained from a Pulse Sensor probe (reflection mode) (*http://pulsesensor.myshopify.com/*). Again, the output was connected to a Shimmer via an expansion board.

2.3 Respiratory rate device

To validate the respiratory rate derived from the IR PPG signal, we built a respiratory measurement circuit. The circuit measured the temperature fluctuations during the breathing phases using a thermistor inserted into a nasal cannula. The resistance of the thermistor decreased when the local temperature increased during expiration, and the resistance increased during inspiration. The thermistor was connected to a voltage divider circuit. The output voltage was connected to an Easy Pulse board to record the temperature fluctuation.

The schematic of the entire monitoring system (respiratory circuit and PPG sensor) is shown in Fig. 2.

Fig. 2. Block diagram of the system

The expansion board from Shimmer allows two analog input connections, which were used for the IR PPG signal and the thermistor signal.
The PPG and reference signal were recorded at a sample frequency of 102.4 Hz.

2.4 Derivation of the respiratory rate from PPG signals

A. PPG features

We developed a Matlab code that extracted several features from the PPG signal, from which the respiratory rate was estimated. The variation of each feature highly represents the respiratory signal. From this signal we extracted the respiratory rate by counting the individual peaks. Fig. 3 describes the PPG features.

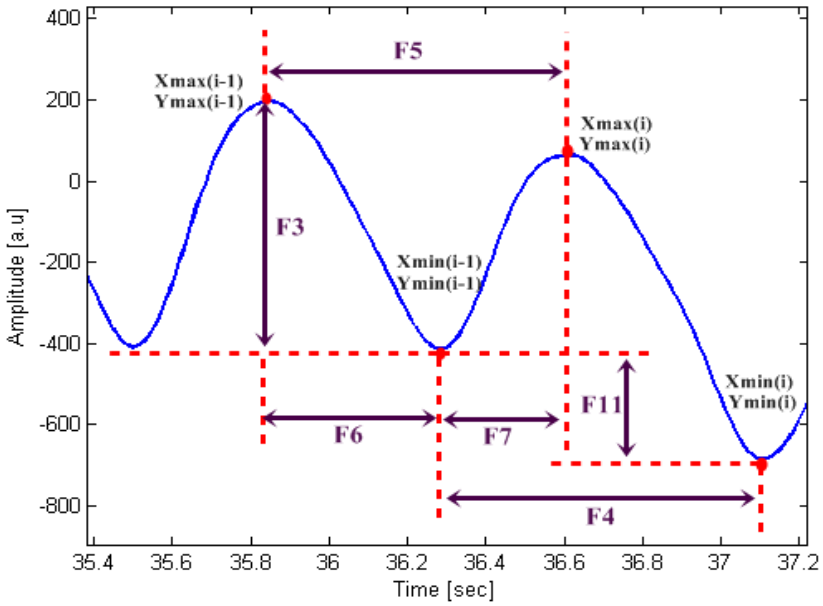

Fig. 3. PPG features

We included the common features PAV, PWV, PRV, PPG envelope and FFT as they have already been evaluated by other researchers [19]. Feature F1 is ymax (upper envelope) and feature F2 is the lower envelope (ymin). PAV is feature F3 as illustrated in Fig. 2, which is defined as

$$F3 = ymax(i) - ymin(i). \quad (1)$$

PWV is feature F4 and is defined as

$$F4 = xmin(i) - xmin(i-1). \quad (2)$$

PRV is feature F5, defined as

$$F5 = xmax(i) - xmax(i-1). \quad (3)$$

In addition we introduced the following features:

$$F6 = xmin(i) - xmax(i), \quad (4)$$

$$F7 = xmax(i) - xmin(i-1), \quad (5)$$

$$F11 = ymin(i) - ymin(i-1). \quad (6)$$

Furthermore, feature F8 is the total area under a PPG peak waveform, feature F9 is the ascending area (area under the PPG signal until the maximum), and feature F10

the descending area. Lastly, feature F12 is the location of the respiratory peak in the Fourier spectrum of PPG signal. The respiratory peak was identified by finding the maximum amplitude peak in the range of 0.1 – 0.8 Hz.

B. Validation

To validate the respiratory rate features we used nine simultaneous PPG and respiratory records from the online database CapnoBase.org [32]. These records are from children between 1 and 8 years old and all are recorded over 8 minutes. For every minute of the PPG signal we extracted the respiratory signal from all the features and computed the respiratory rate by counting the number of peaks. The counting was performed using a peak detection algorithm. Using this algorithm we searched for the highest point, around which there are points lower by "X" on both sides. In total we had 72 points for every feature (9 records x 8 minutes = 72). We also determined the respiratory rate from every minute of the respiratory signal (the flow) and used these values as a reference.

C. Bland Altman Plot

The Bland Altman plot was used to evaluate the best features. For all the 12 features we made a Bland Altman analysis to identify the mean (MD) and standard deviation (SD) of the differences between the respiratory rates obtained from the features and the reference measurement. A good feature should provide a respiratory rate estimate with a small MD and SD. We made a bar graph to compare the results from all features.

D. Majority rule algorithm

After selecting the best features from Bland Altman analysis, we applied the "Majority rule" algorithm, to obtain the final respiratory rate value derived from the PPG signal. The steps in this algorithm are described below.

1. Extraction of respiratory signal (variation of each feature in time)
2. Compute the respiratory rate from every feature
3. Apply outlier removal: rates deviating more than one standard deviation from the median were removed
4. Identify the unique values and how many times each value appears
5. If more than half of the computed respiratory rates have the same value, then this will be the final value displayed. If not, the final respiratory rate will be the rounded mean of the values remaining after outlier removal.

E. Measurements on the volunteers

For our study we tested the extraction algorithm on four young volunteers: three women and one man. We performed several measurements on different sites of the body such as upper arm, wrist and ankle. In this paper the results from the upper arm measurements are shown in detail. We chose the upper arm because is a location where monitoring armbands can be placed. In comparison, the wrist is sensitive at

motion artefacts, and the ankle is not usually used in monitoring. Every record had a length of 5 minutes. During the recordings, all the volunteers stayed in sitting position and the room temperature was 25^{o}C.

F. **Test the accuracy of the real-time extraction algorithm**

To test the accuracy of the algorithm, we computed the un-normalized root mean square (RMS) error. The RMS error was calculated for every record, considering all respiratory rate estimations over 5 minutes:

$$RMS = \sqrt{\frac{1}{n}\sum_{i=1}^{n}(x(i)ref - x(i)ppg)^2} \tag{7}$$

where n=5, x(i)ref is the respiratory rate from the reference and x(i)ppg is the respiratory rate from ppg signal.

3 Results and Discussion

3.1 Evaluation of the features.

Before the real-time measurements, we tested the algorithm on signals from the CapnoBase database. The respiratory signal (flow) was used as a reference for the respiratory waveform obtained from the PPG features.

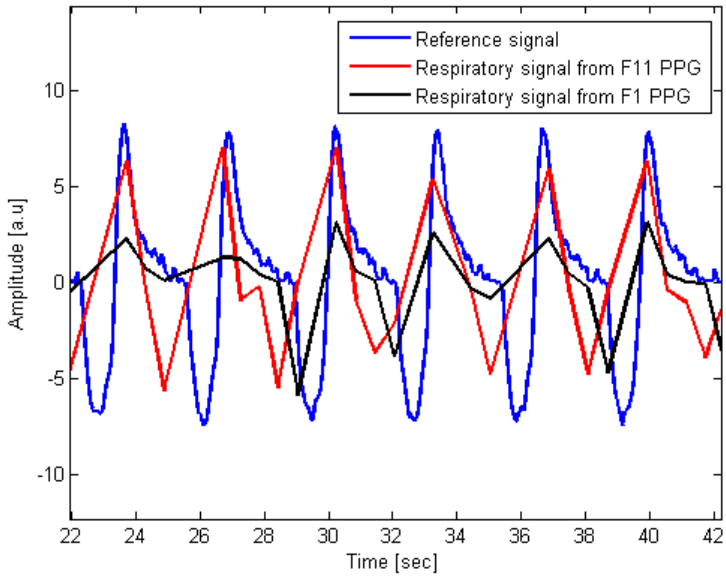

Fig. 4. A segment of reference signal and respiratory signal extracted from F1 and F11

Fig.4 shows a one-minute data segment of a reference respiratory signal (blue), and two derived respiratory signals based on feature F1 (black) and feature F11 (red). The mean has been subtracted from every signal. We can observe that PPG-derived respiratory signals have strong correlation with the reference signal. The new feature introduced, F11, compares better to the reference signal than Upper Pulse Envelope (F1). We used a peak detection algorithm to count the peaks. Using this number we can compute the respiratory rate.

We also computed the respiratory rate from the PPG signal using the classic FFT analysis. Fig. 5 illustrates the result from the FFT analysis, where the peak at 0.3 Hz corresponds to the respiratory frequency (18 breaths/min), and the maximum at 1.7 Hz gives us information about the heart rate (101 beats/min). The respiratory rate computed via this method has the same value as the reference and the respiratory rate derived from the features.

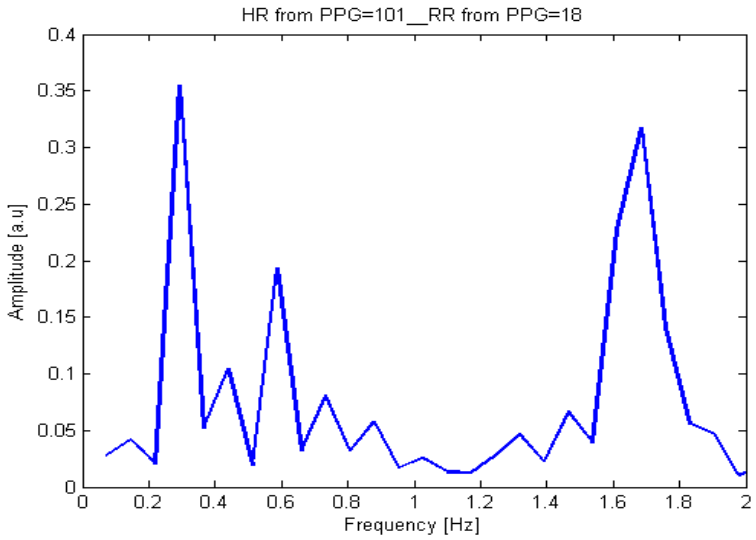

Fig. 5. Frequency spectrum of PPG signal

3.2 Evaluation of the Bland Altman plot and the Majority Rule

To determine which features provided the most accurate estimate of the respiratory rate, we analyzed the MD and SD corresponding to each of the features via Bland Altman plots. The Bland Altman plot for feature 11 (Fig. 6) illustrates a confidence interval between -2 and 2 and a negligible bias.

The bar graph of the MDs and SDs (Fig. 7) shows that F1, F3, F4 and F11 have MDs smaller than 0.5 breath/min and F1, F2, F3, F11 have SDs smaller than 1.5 breath/min.

We chose the features F1, F2, F3, F4, F11, because they have smallest MD and SD. These features will be used in the majority rule to compute the final respiratory rate.

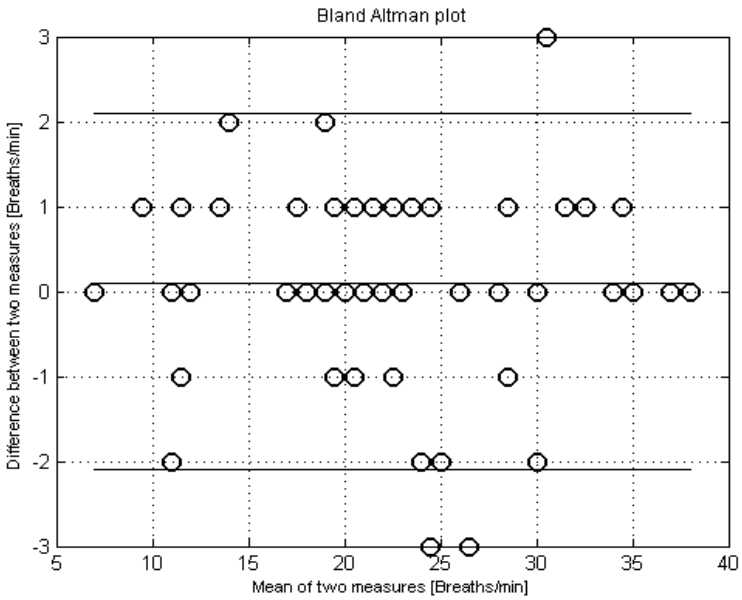

Fig. 6. Bland Altman plot of feature F11

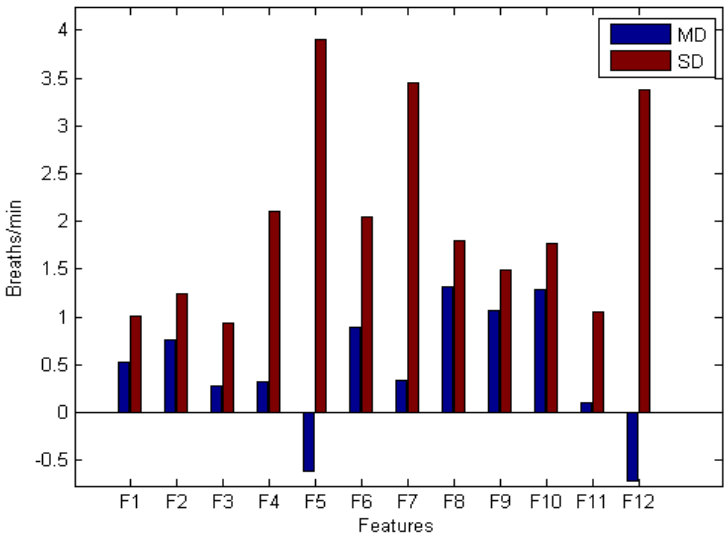

Fig. 7. MD and SD bar graph

The majority rule algorithm allowed us to extract the respiratory rate from the PPG signal, considering all the information provided by the selected features. We used this fusion method to increase the stability of the system, reduce the errors and improve the estimation of respiratory rate.

3.3 Real-time measurements.

We performed several recordings with the PPG sensor placed on the upper arm and the thermistor circuit under the nose, to see how the algorithm performs in real-time, at different respiratory frequencies. The processing has been performed on a 1-minute buffer.

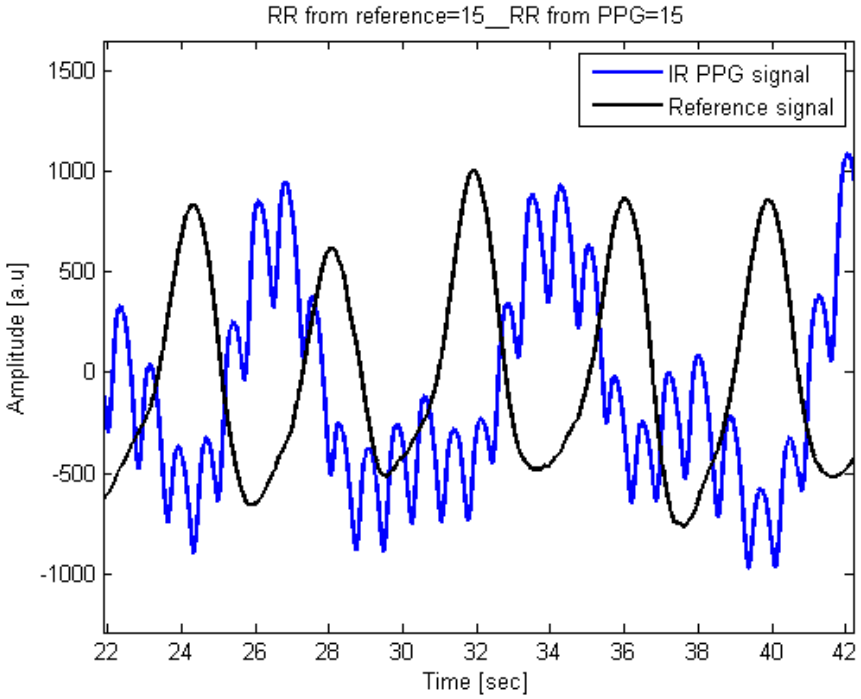

Fig. 8. Real time recording of IR PPG signal and reference signal

Figure 8 presents the results from the real-time extraction of the respiratory rate from the IR PPG signal and the reference signal.

Figure 9 shows the respiratory waveforms derived from feature F1 (black) and F11 (red) and the reference (blue), at different respiratory frequencies.

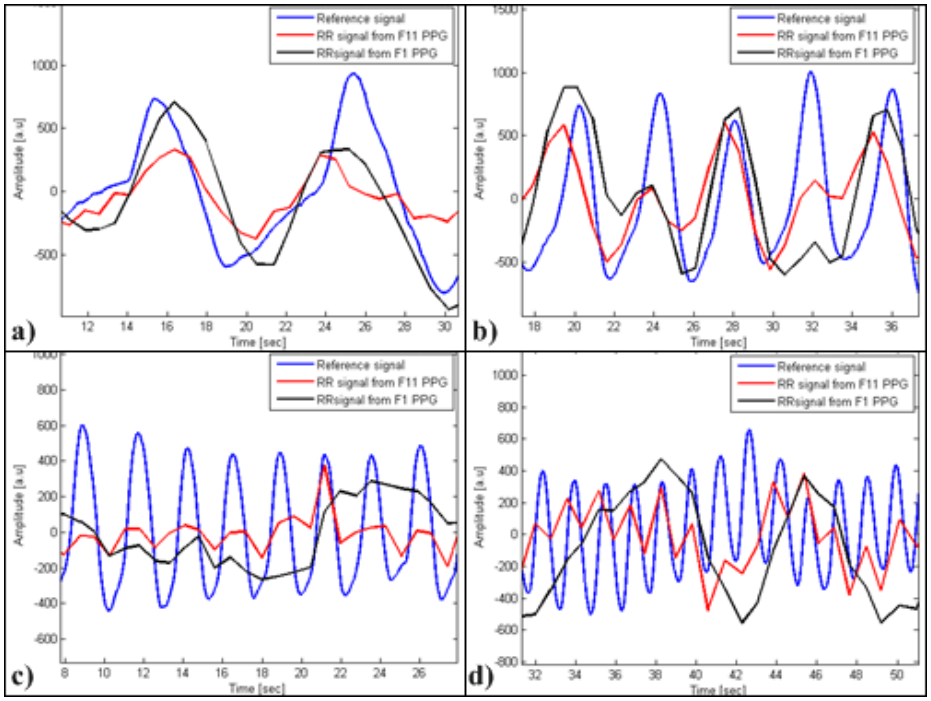

Fig. 9. Time traces of features F1 (black) and F11 (red) and the reference (blue), at different respiratory frequencies:

a) 6 breaths/min; b) 15 breaths/min; c) 24 breaths/min; d) 42 breaths/min

As it can be seen, at low and normal respiratory rates (Fig. 9 a and b), the respiratory signals derived from both features coincide with the reference signal. When the respiratory rate increases, exceeding values over 30 breaths per minute the respiratory waveforms estimated from the PPG signal do not longer accurately show the respiratory rate. This is due to the fact that the changes caused by breathing can no longer be seen in PPG signal at higher rates. However, the new feature introduced shows a resemblance with the reference trace even at higher frequency. When the respiratory rate was between 40 and 45 breaths/minute, we obtained an error of 6 breaths/minute.

In Table 1 the results for the upper arm recordings, performed on the volunteers, are presented. After computing the respiratory rate for every minute of the record, we calculated the average (M) and standard deviation (Std) of the respiratory rate extracted from the PPG and reference signal and RMS error. At low and normal respiratory frequencies the RMS error is between 0.77 – 1.41 breaths/minute. As the respiratory rate increases, the algorithm do not longer give accurate results, the RMS error exceeding values over 10 breaths/minute when the respiratory rate is above 40 breaths/min. We performed various recordings by placing the PPG sensor on different sites of the body (Figure 10).

No. subj	Respiratory rate range														
	low					medium					high				
	M		Std		RMS	M		Std		RMS	M		Std		RMS
	Ref	PPG	Ref	PPG		Ref	PPG	Ref	PPG		Ref	PPG	Ref	PPG	
1	7.4	8.2	1.51	0.83	1.09	13.6	13	0.55	1.41	1.18	39.4	32	3.84	2.88	10
2	7.2	7.8	0.45	0.84	1	15.4	15.2	1.52	1.09	0.77	34.6	29.4	1.34	2.3	5.86
3	9	9.4	0.71	1.52	1.26	12.4	13.2	0.54	1.30	1.41	43	27	5.31	1.87	17.34
4	8	9	0.71	0.71	1	14.8	13.6	1.3	1.52	1.26	28.8	25.6	2.17	1.67	3.28

Table 1. Average, standard deviation and RMS error of the respiratory rate extracted from the PPG signal from upper arm. M represent the mean respiratory rate, Std ist he standard deviation and RMS ist he root mean squred error. The unit of measurement for M and RMS is breaths/minute.

Left Upper Arm

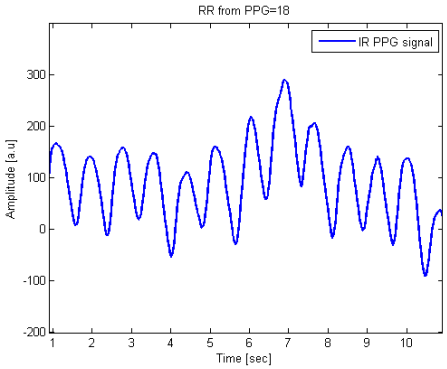

Right Upper Arm

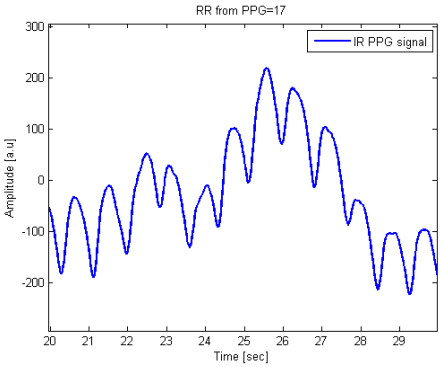

Left Wrist

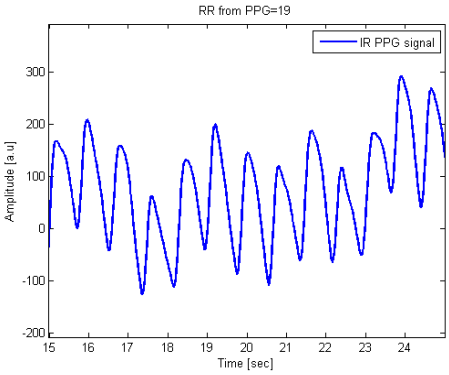

Right Wrist

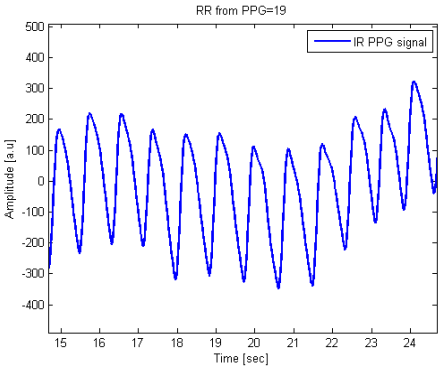

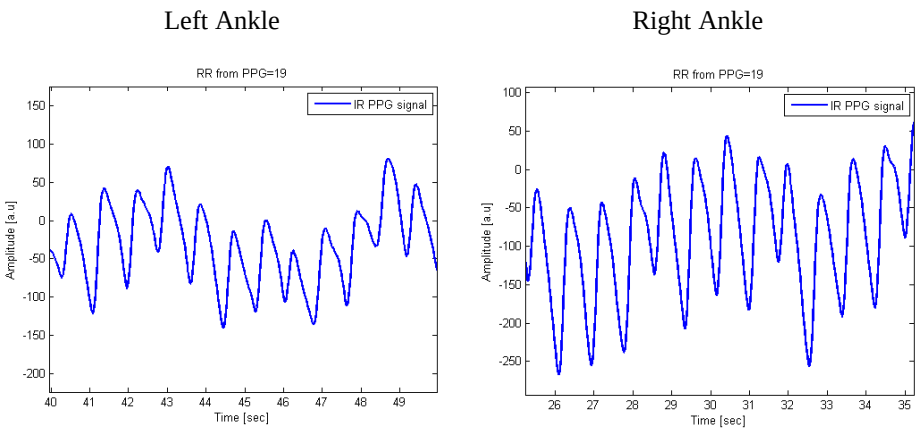

Fig. 10. PPG signal with Respiratory rate extraction from different sites of the body.

The same measurements have also been done using a green PPG sensor that works in reflection mode. Using the same features (F1, F2, F3, F4 and F11) and the fusion rule described above we managed to extract the respiratory rate from the green PPG signal, with the same error range as obtained when using the IR PPG signal.

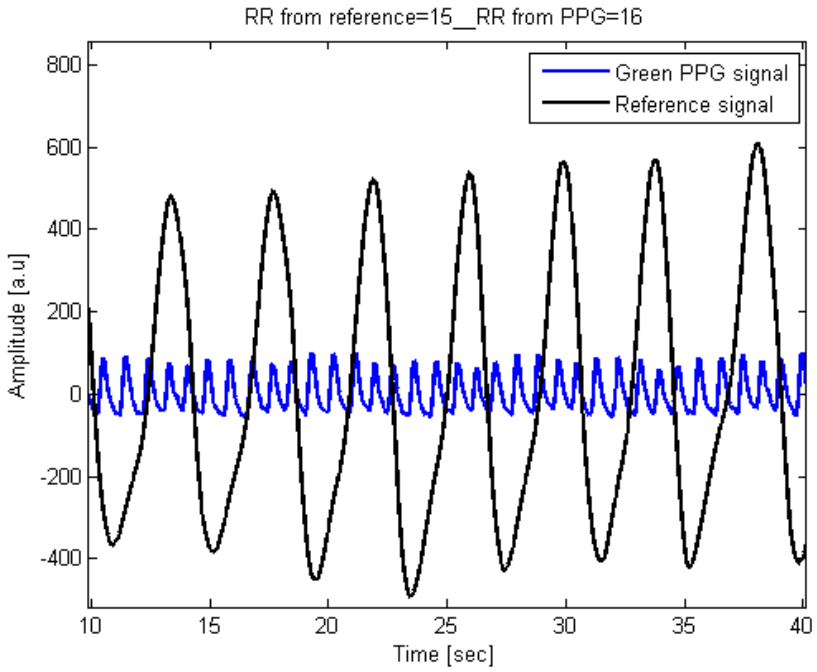

Fig. 11. Respiratory rate extraction from Green PPG

For both the green and IR PPG signals, the extracted respiratory rate showed large errors at high respiratory rates (>6 breaths). This was a result of the diminished observability of the peaks in the respiratory signals, which were observable at lower respiratory rates. It is possible that at this high frequency the PPG signal cannot capture the respiratory modulation. However, this will require further research.

4 Conclusions

We have showed that more features can be derived from PPG signals to determine the respiratory rate, in addition to PAV and PWV. From the features presented above, feature F11, which capture the fluctuations of the DC signal, provides results comparable to the most commonly features used in the literature (PAV, PWV). Our approach to extract the respiratory frequency is simpler than the one using FFT. This is because we use the same code to count the peaks in the respiratory signal as the one for extracting heart rate. The data fusion algorithm we proposed provided better results in real time when compared with a flow circuit. The error was maximum 2 breaths/minute for respiratory frequencies between 6 and 30 breaths/minute. For higher respiratory frequencies the modulations induced by respiration in the PPG are smaller and this will be a point to address in future.

In addition we showed that we successfully extract the respiratory rate from different location of the body such as the upper arm, wrist and ankles. Moreover, the extraction performed using either IR or green PPG signals provided similar results. The new algorithm can be embedded in wearable devices to allow recording of both the respiratory rate and the heart rate. Furthermore, this type of data can be used to monitor cardiorespiratory coupling in medical conditions such as epilepsy.

References

1. F.Q. AL-Khalidi, R. Saatchi, D. Burke, H. Elphick, and S. Tan , “Respiration rate monitoring methods: A review”, *Pediatric Pulmonology*, vol 46, no.6, pp. 523-539, June 2011.
2. W. Karlen, S. Raman, J.M. Ansermino, G.A. Dumont, “Multiparameter Respiratory Rate Estimation From the Photoplethysmogram”, *IEEE Transactions on Biomedical Engineering*, vol. 60, no. 7, pp. 1946-53, July 2013.
3. G. Yuan, N.A. Drost, R.A. Mclvor, “Respiratory Rate and Breathing Pattern”, MUMJ – *Clinical Review*, vol. 10, no.1, pp.23-25, 2013.
4. L. Hans, Y. Mawji, “The ABCs of Emergency Medicine”,Twelfth Edition, 2012, Faculty of Medicine, University of Toronto.
5. M. Seyal, L.M. Bateman, T.E. Albertson, T.C. Lin, C.S. Li, “Respiratory changes with seizures in localization-related epilepsy: analysis of periictal hypercapnia and airflow patterns.” *Epilepsia*, vol.51, no.8, pp. 1359-64, August 2010 .

6. R. Kloster, T. Engelskjøn, "Sudden unexpected death in epilepsy (SUDEP): a clinical perspective and a search for risk factors", *J. Neurol Neurosurg Psychiatry*, vol. 67, no.4, pp. 439-444, 1999.
7. P. Ryvlin, L. Nashef , S.D. Lhatoo, L.M. Bateman et al., "Incidence and mechanisms of cardiorespiratory arrests in epilepsy monitoring units (MORTEMUS): a retrospective study", *The Lancet Neurology*, vol.12, no. 10, pp. 966-977, October 2013.
8. G.B. Drummond, A.F. Nimmo, R.A. Elton, "Thoracic impedance used for measuring chest wall movement in postoperative patients", *British J of Anaesthesia*, vol.77, no.3, pp. 327-332, June 2011.
9. P. S. Addison, J. N. Watson, M. L. Mestek, and R. S. Mecca, "Developing an algorithm for pulse oximetry derived respiratory rate (RR(oxi)): a healthy volunteer study.," *J. Clin. Monit. Comput.*, vol. 26, no. 1, pp. 45–51, Feb. 2012.
10. L.G. Lindberg, H. Ugnell, P.A.Oberg, "Monitoring of respiratory and heart rate using a fibre-optic sensor", *Med. & Biol. Eng. & Comput*., vol.30, no.5, pp. 533-537, 1992.
11. W.S. Johnston, Y. Mendelson, "Extracting breathing rate information from a wearable reflectance pulse oximeter sensor", *Conf Proc IEEE Eng Med Biol Soc* , vol. 7, pp. 5388-91, 2004
12. D. Barschdorff, W. Zhang, "Respiratory rhythm detection with photoplethysmographic methods", *Proceedings of the 16th Annual International Conference of the IEEE*, vol.2, pp. 912 - 913, November 1994
13. L. Nilsson, A. Johansson, and S. Kalman, "Respiration can be monitored by photoplethysmography with high sensitivity and specificity regardless of anaesthesia and ventilatory mode," *Acta Anaesthesiol. Scand*., vol. 49, no. 8, pp. 1157–62, Sep. 2005
14. L. Nilsson, T. Goscinski, A. Johansson, L. G. Lindberg, and S. Kalman, "Age and gender do not influence the ability to detect respiration by photoplethysmography," *J. Clin. Monit. Comput.*, vol. 20, no. 6, pp. 431–6, Dec. 2006.
15. K. Nakajima, T. Tamura, and H. Miike, "Monitoring of heart and respiratory rates by photoplethysmography using a digital filtering technique," *Med. Eng. Phys.*, vol. 18, no. 5, pp. 365–72, Jul. 1996.
16. P. Addison and J. Watson, "Secondary wavelet feature decoupling (SWFD) and its use in detecting patient respiration from the photoplethysmogram," in *Engineering in Medicine and Biology Society. Proceedings of the 25th Annual International Conference of the IEEE*, Sep. 2003, pp. 2602–5.
17. P. Addison, J. N. Watson, M. L. Mestek, J. P. Ochs, A. A. Uribe, S. D. Bergese, "Pulse oximetry-derived respiratory rate in general care floor patients", *J Clin Monit Comput*, pp.1-8, may 2014.
18. S.G. Fleming, L. Tarassenko, "A Comparison of Signal Processing Techniques for the Extraction of Breathing Rate from the Photoplethysmogram", *International Journal of Medical, Health, Pharmaceutical and Biomedical Engineering*, vol.2, no.4, pp. 232-236, 2007.
19. J. Lazaro, E. Gil, R. Bailon, P. Laguna, "Deriving respiration from the pulse photoplethysmographic signal", *Computing in Cardiology*, vol.38, pp. 721-716, 2011.
20. Y. Mendelson , M. J. McGinn, "Skin reflectance pulse oximetry: In vivo measurements from the forearm and calf", *Journal of Clinical Monitoring*, vol.7, no.1, pp. 7-12, January 1991.
21. R Bailo, L. Sornmo, P. Laguna, "A robust method for ecg- based estimation of the respiratory frequency during stress testing", *IEEE Transactions on Biomedical Engineering*, vol.53, no.7, pp. 1273-85, 2006.
22. V. Kamat, " Pulse Oximetry", *Indian J Anaesth*, vol.46, no.4, pp.261-268, 2002.

23. P. D. Mannheimer, "The light-tissue interaction of pulse oximetry.," *Anesth. Analg.*, vol. 105, no. 6 Suppl, pp. S10–7, Dec. 2007.
24. W.W. Hay, Jr., D.J Rodden , S.M. Collins, D.L. Melara, K.A.Hale, L.M. Fashaw, "Reliability of conventional and new pulse oximetry in neonatal patients", *J Perinatol*, vol.22, no.5, pp.360-366, Jul-Aug 2002.
25. A. Sola, L. Chow, M. Rodigo, "Pulse oximetry in neonatal care in 2005. A comprehensive state of the art review", An Pediatr ,vol. 62, no.3, pp. 266 – 280, 2005.
26. Y. Mendelson, "Pulse Oximetry: Theory and Applications for Noninvasive Monitoring", Clinical Chemistry,vol. 38, no. 9, pp. 1601-7, 1992.
27. J. Allen, "Photoplethysmography and its application in clinical physiological measurement", *Physiological Measurement*, vol.28, no.3, pp. 1-39, 2007.
28. D.J Meredith, D. Clifton, P. Charlton, J. Brooks, C.W. Pugh, et al., "Photoplethysmographic derivation of respiratory rate: a review of relevant physiology", *Journal of Medical Engineering & Technology*, vol.36, no.1, pp.1–7, 2012.
29. Y. Mendelson, B.D. Ochs, "Noninvasive pulse oximetry utilizing skin reflectance photoplethysmography", *IEEE trans Biomed Eng*, vol. 35, no. 10, pp. 798-805, Oct 1988.
30. R. G. Haahr, S. B. Duun, M. H. Toft, B. Belhage, J. Larsen, K. Birkelund, and E. V Thomsen, "An Electronic Patch for wearable health monitoring by reflectance pulse oximetry.," *IEEE Trans. Biomed. Circuits Syst.*, vol. 6, no. 1, pp. 45–53, Feb. 2012.
31. S. Ciorecan, C. Ungureanu, M. Ungureanu, R. Aarts, J. Arends, " A new design of reflectance pulse oximeter", to be submitted.
32. W. Karlen., M. Turner, E. Cooke, G.A. Dumont, and J.M. Ansermino, "CapnoBase: Signal database and tools to collect, share and annotate respiratory signals*", Proc. Annu. Meet. Soc. Technol. Anesth*., West Palm Beach, FL, USA, 2010, pp. 2